Univerzitet u Beogradu
Poljoprivredni fakultet
Institut za poljoprivrednu tehniku
Naučni časopis
POLJOPRIVREDNA TEHNIKA
Godina L
Broj 1., 2025.
Strane: 76 – 88

University of Belgrade
Faculty of Agriculture
Institute of Agricultural Engineering
Scientific Journal
AGRICULTURAL ENGINEERING
Year L
No. 1., 2025.
pp. 76 – 88

Original Scientific paper
Originalni naučni rad
DOI: 10.5937/POLJTEH2501076F

NUMERICAL MODELING OF TURBO PNEUMATIC SIEVING PROCESS FOR BAMBARA FLOUR PRODUCTION USING COMPUTATIONAL FLUID DYNAMICS

Ijeoma Francisca Ikechukwu*[1], Awa David Onwuka[1], Onyekachukwu James Nwosu[2]

[1]Department of Mechanical Engineering, Michael Okpara University of Agriculture, Umudike, Nigeria
[2]Department of Mechanical Engineering, Gregory University, Uturu, Abia State, Nigeria

Abstract. The semi mechanized method used in Bambara flour processing in sub-Sahara Africa remain a major bottleneck in the utilization of Bambara nuts. In this study, a numerical model was used to study and predict the flow characteristics in a turbo pneumatic sieving chamber of a novel Bambara flour processing machine. For this purpose a Computational Fluid Dynamics model was employed. As a result, shearing stress, transport, large and eddy simulation turbulence models were tested in order to improve the model. For the simulation of the sieve effect, a porous domain was used. The pressure, velocity of fluid and also the turbulence areas were analyzed. The result of the analyses using Computational Fluid Dynamics shows the fluid flow and particles motion within the sieving chamber with a normal distribution of total pressure, it also revealed that the sieving process is greatly affected by the pressure, air velocity stream and the turbulence kinetic energy inside the sieving chamber. The invaluable insight gleaned from this research on the effect of pressure, air velocity stream and the turbulence kinetic energy in the sieving processes of bambara flour will serve as a corner stone for informing and optimizing future design iterations, ultimately revolutionizing the field and driving innovation

Keywords*: Bambara flour, Computation Fluid Dynamics, simulation, flow pattern, pneumatic Sieving*

*Corresponding Author. E-mail: ikechukwuijeoma7@gmail.com
ORCID: 0000-0002-8728-0396

INTRODUCTION

Impact analyses conducted in sub-Saharan Africa have demonstrated that the cultivation of native legume crops can effectively mitigate the susceptibility of rural households to food and nutrition instability. An example of such a legume is the Bambara nut (*Vigna subterranean*), which is commonly found in subsistence farming systems across semi-arid regions of Sub-Saharan Africa [1, 3]. According to [1], Bambara nut is a valuable and affordable source of protein in diets, particularly in regions where animal protein is rather costly, as mentioned in [2]. The crop has a higher protein score (80%) than soya beans (74%) and cowpeas (64%), and it is richer in essential amino acids than other legumes [3]. These findings suggest that Bambara nut contains a higher amount of protein that may be readily used by the human body compared to other commonly consumed legumes. Bambara nut has been used in various ways by producing communities in Nigeria. Every group has its unique method of cooking the bambara nut delicacy for consumption. The nut is frequently utilised in food preparation, where it is transformed into flour and employed in the making of soup, porridge, and a variety of fried or steamed dishes such as 'akara', 'moi-moi', and 'okpa', [4]. The newly harvested pods are also cooked in boiling water with salt and pepper and consumed as a snack [5]. Furthermore, it has been shown that in the northeastern region of Nigeria, bambara groundnut serves not only as a dietary staple but also possesses therapeutic properties. The results gained from this experiment have confirmed the efficacy of computational fluid analysis in modelling. The manual milling and sieving procedure of Bambara groundnut has recently become a significant obstacle in the efficient use of Bambara nuts [6]. Currently in Nigeria, the process of separating ground bambara flour still relies on manual labour, save for the involvement of [7] who created a turbo pneumatic milling and sieving machine specifically for this purpose. However, this machine has not been widely adopted by processors. Ground bambara flour contains both undesired or coarse particles and fine particles that are mixed together during the milling process. These particles can be separated using a sieve procedure. The screening procedure is essential for separating the fine flour of ground Bambara nuts from the fibrous material of the seed coat and the flour that is produced when the milling operation is not sufficient. To enhance the particle flow pattern in the sieving chamber, this work focuses on applying computational fluid dynamics (CFD) to numerical modelling of the bambara nut milling and sieving machine's turbo pneumatic sieving process.

Extensive research has been conducted on the utilisation of Computational Fluid Dynamics (CFD) in several domains. [8, 9, 10, 11] conducted a review on the use of computational fluid dynamics (CFD) in the ventilation of agricultural buildings. The selection of a turbulent model was found to be a crucial determinant in achieving accurate simulation results, and therefore, it should be made with great care. As analyzed in "Concept of Computational Fluid Dynamics (CFD) and its Applications in Food Processing Equipment Design" evaluated the use of CFD in food processing equipment design, according to [12, 13, 14, 15, 16]. Their research findings demonstrated that Computational Fluid Dynamics (CFD) can serve as a valuable tool for designing food processing equipment. However, the effectiveness and practicality of the system rely on other aspects such as robust CFD software, high-performance computers, and knowledgeable CFD specialists.

Also, [17, 18, 19, 20] conducted a study to demonstrate the practical use of Computational Fluid Dynamics Modelling in the process of heat pump drying of bananas The numerical simulation revealed that the temperature exhibited a consistent decline (from 30.1 to 29.4) similar to the experimental findings of the heat pump dryer being investigated. The study employed simulations to replicate scenarios where obtaining precise measurements is not feasible. [21, 22, 23, 24] performed a computational fluid dynamics (CFD) analysis on the energy and exergy aspects of thin layer drying of okra (abelmoschus esculentus) slices. They utilised a centre shaft rotating tray cabinet (CSRTC) dryer for their study. The Ansys 14.5 Workbench software was utilised to simulate the 2D (2 Dimensional) dryer model. The CFD simulation results were utilised to examine the energy and exergy of the dryer at three different drying temperatures (50, 60, and 70 °C). The simulated temperature from the experiment was seen to be higher than the actual temperature of the experiment. The results demonstrated that the experimental energy utilisation (EU), energy utilisation ratio (EUR), and energy efficiency increased from 14.1 to 57.93 J/s, 0.15 to 0.20, and 18.89 to 33.98 percent, respectively. Similarly, the simulated energy utilisation ratio increased from 23.91 to 57.68 J/s, the energy utilisation ratio increased from 0.19 to 0.20, and the energy efficiency increased from 26.21 to 33.40 percent. These changes occurred as the drying air temperature increased from 50 °C to 70 °C. The experimental exergy inflow increased from 4.01 J/s to 6.98 J/s, the exergy outflow increased from 1.83 J/s to 1.9 J/s, the exergy loss increased from 3.18 J/s to 5.07 J/s, and the exergy efficiency improved from 21% to 27%. Similarly, the simulated air temperatures increased from 5.01 J/s to 7.49 J/s, from 1.33 J/s to 2.20 J/s, from 3.66 J/s to 5.29 J/s, and the exergy efficiency increased from 27% to 29%. These changes were observed within the drying air temperature range of 50-70 °C. [25, 26] Carried out a study to demonstrate the utilisation of computational fluid dynamics (CFD) in simulating the flow profile and temperature distribution of hot air in a cech dryer. Their research shown that the turbulence model employed in the computational fluid dynamics (CFD) simulation has the ability to accurately forecast the dynamic characteristics of the dryer. Therefore, Computational Fluid Dynamics (CFD) is exceptionally effective in forecasting the flow of air and analysing the characteristics related to drying. The results produced from the computational fluid analysis demonstrate its efficacy in modelling, which led to its acceptance for this study. This task was facilitated by a computer system equipped with ANSYS and SolidWorks software, which assisted in the design and analysis process. The design was created using SolidWorks 2013 and then exported to ANSYS. The model was specifically built for simplicity of simulation, as the ANSYS Fluent solver utilises a cell-centered finite volume approach to analyse and discretize models. Figure 1 depicts the visual representation of the ANSYS model of the sieving chamber of the machine. The article discusses several steps to achieve efficient results in ANSYS, which are outlined under the following headings [27, 28].

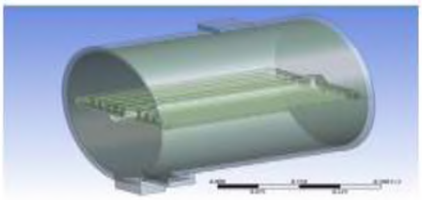

Fig.1. ANSYS model of the Sieving chamber

Geometry Import

The ANSYS Geometry tools are specifically engineered to offer robust computer aided design (CAD) neutral capabilities to users of the complete suite. These tools allow users to import, repair, alter, simplify, and construct geometry from nearly any CAD source. Additionally, users can transfer the same geometry to any of the ANSYS meshing products. The ANSYS Geometry tools are specifically designed to minimize the time required to create a precise simulation model.

Meshing

Meshing is the procedure of transforming irregular shapes into well-defined volumes known as elements. Meshing begins after a geometry or CAD model is uploaded into ANSYS. Meshing is the procedure by which the continuous geometric space of an object is divided into numerous smaller shapes to accurately represent the physical shape of the thing. ANSYS meshing capabilities expedite the acquisition of simulation results by providing superior and highly automated meshing tools.

Setup

Once you have generated a computational mesh for the geometry, you can move to configuring a computational fluid dynamics (CFD) analysis using ANSYS FLUENT within the ANSYS workbench. This will then lead to the subsequent phase of executing the calculations, known as the solution stage.

Solution

The solution methods task page enables you to define several parameters related to the solution method that will be employed in the calculation. Within the ANSYS Mechanical software, A folder named "solution information" is utilised for the solution. By selecting the solution information branch in the solution, the graphics window transitions into the worksheet window, where you may view the output generated by the solver. The file generated by ANSYS Mechanical APDL during the solving process contains valuable data. The window refreshes at a duration specified by the user, and the default period of 2.5 seconds appears to be effective. It is advisable, even for a non-changing process, to monitor this window as things are resolved. It provides information about the current position of the solver in the solving process. Additionally, it displays any potential warnings and provides a comprehensive list of information regarding your model and solver configurations.

Nomenclature

ρ = Fluid density (unit: W/m^2)
U = Vector of velocity
t = Time (unit: seconds))
τ = Shear stress (unit: Pa)
P = Static (thermodynamic) pressure (Unit: Pa)
S_M = Momentum source
μ = Molecular (dynamic) viscosity
T = Static (thermodynamic) temperature
δ = Identity matrix function

h_{tot} = Specific total enthalpy
h = Thermal conductivity
S_E = Energy source
W = Molecular weight
p_{abs} = Absolute pressure, and is the universal gas constant. (Unit: pa)
k = turbulence kinetic energy per unit mass
μ_τ = Turbulent viscosity
σ_k = Turbulence model constant for the turbulent kinetic energy equation
β = Coefficient of thermal expansion
ω = Angular velocity
σ_ω = K-ω turbulence model constant
u_p = Particle velocity
ρ_p = Particle density
d_p = Particle diameter
Re_p = Particle Reynolds number

MATERIAL AND METHODS

A CFD-DPM coupling model was utilized to simulate the fluid flow within the sieve chamber. The fluid flow inside the sieving chamber is turbulent and unsteady due to the spinning of the shaft and paddles. Equations 1 through 4 were used to calculate the continuity equation, momentum equations, total energy equation, and ideal gas equation of state for the computation of fluid flow in a turbulent flow [28];

The continuity equation:

$$\frac{\partial\rho}{\partial t} + \nabla\cdot(\rho U) = 0 \qquad \text{...... (1)}$$

The momentum equation:

$$\frac{\partial(\rho U)}{\partial t} + \nabla\cdot(\rho U \otimes U) = -\nabla \mathrm{P} + \nabla\cdot\tau + S_M \qquad \text{...... (2)}$$

Where the stress tensor, is related to the strain rate by:

$$\tau = \mu(\nabla U + (\nabla U)^{\mathrm{T}} - \frac{2}{3}\delta\nabla\cdot U) \qquad \text{.....(3)}$$

The total energy equation:

$$\frac{\partial(\rho h_{tot})}{\partial t} - \frac{\partial\rho}{\partial t} + \nabla\cdot(\rho U_{tot}) = \nabla\cdot(\lambda\nabla T) + \nabla\cdot(U\cdot\tau) + U\cdot S_M + S_E \qquad \text{..... (4)}$$

Where h_{tot} is the total ethalpy, related to the static enthalpy h (T, ρ) by:

$$h_{tot} = h + \frac{1}{2}U^2$$

The expression ∇·(U·τ) denotes the energy expended as a result of viscous strains and is referred to as the viscous work term. The contribution of internal heating due to viscosity in the fluid is insignificant in the majority of flows. Furthermore, the word U·S_M denotes the contribution of an external momentum source and is now disregarded.

The density of an ideal gas can be determined using the Ideal Gas law and is mostly dependent on temperature, as described by equation (5);

$$\rho = \frac{w p_{abs}}{R_0 T}$$
$$dh = c_p dT \qquad \text{......(5)}$$
$$c_p = c_p(T)$$

A shear stress transfer (SST) turbulent model was utilised for this investigation. The SST model can be understood as an enhanced version of the Baseline (BSL) k-Omega turbulent model. When using the Wilcox k-Omega turbulent model, it was shown that the stated value of ω at the inlet might lead to large variations in the model's output. In order to address the issue, a hybrid model was devised that combines the k-ω model on the surface with the k-ε model in the outer region. The process involves converting the k-ε model into a k-ω formulation and then incorporating the relevant equations. The Wilcox model is multiplied by a blending functionF_1, while the converted k-ε model is multiplied by a function$(1 - F_1)$.
The value of F_1 is equal to one near the surface and gradually declines to zero outside the boundary layer, following a function of the wall distance as shown in equation 6 to 7.
The Wilcox (k-ω) model:

$$\frac{\partial(\rho k)}{\partial t}+\frac{\partial}{\partial x_j}(\rho U_j k)=\frac{\partial}{\partial x_j}\left[\left(\mu+\frac{\mu_\tau}{\sigma_{k1}}\right)\frac{\partial k}{\partial x_j}\right]+p_k-\beta'\rho k\omega$$

$$\frac{\partial(\rho\omega)}{\partial t}+\frac{\partial}{\partial x_j}(\rho U_j \omega)=\frac{\partial}{\partial x_j}\left[\left(\mu+\frac{\mu_\tau}{\sigma_{\omega1}}\right)\frac{\partial \omega}{\partial x_j}\right]+\alpha_1\frac{\omega}{k}p_k-\beta'\rho k\omega^2 \qquad ....(6)$$

Transformed k - ε model:

$$\frac{\partial(\rho k)}{\partial t}+\frac{\partial}{\partial x_j}(\rho U_j k)=\frac{\partial}{\partial x_j}\left[\left(\mu+\frac{\mu_\tau}{\sigma_{k2}}\right)\frac{\partial k}{\partial x_j}\right]+p_k-\beta'\rho k\omega$$

$$\frac{\partial(\rho\omega)}{\partial t}+\frac{\partial}{\partial x_j}(\rho U_j \omega)=\frac{\partial}{\partial x_j}\left[\left(\mu+\frac{\mu_\tau}{\sigma_{\omega2}}\right)\frac{\partial \omega}{\partial x_j}\right]+2\rho\,\frac{1}{\sigma_{\omega2\omega}}\cdot\frac{\partial k}{\partial x_j}\cdot\frac{\partial \omega}{\partial x_j}+\alpha_2\frac{\omega}{k}p_k \qquad ....(7)$$

σ = use as a subscript to indicate that the quantity applies to phase

The Wilcox model equations are multiplied by the functionF_1, while the modified k-ε equations are multiplied by the equation$1 - F_1$. The resulting k- and ω- equations are then combined together to create the BSL model. Accounting for the influence of gravity, the fundamental model is represented by equation 8 to 9
The turbulent kinetic energy is described by the transport equation;

$$\frac{\partial(\rho k)}{\partial t}+\frac{\partial}{\partial x_j}(\rho U_j k)=\frac{\partial}{\partial x_j}\left[\left(\mu+\frac{\mu_\tau}{\sigma_{k3}}\right)\frac{\partial k}{\partial x_j}\right]+p_k-\beta'\rho k\omega+p_{kb} \qquad \ldots\ldots (8)$$

Transport equation of the turbulent frequency:

$$\frac{\partial(\rho\omega)}{\partial t}+\frac{\partial}{\partial x_j}(\rho U_j \omega)=\frac{\partial}{\partial x_j}\left[\left(\mu+\frac{\mu_\tau}{\sigma_{\omega3}}\right)\frac{\partial \omega}{\partial x_j}\right]+(1-F)2\rho\,\frac{1}{\sigma_{\omega2\omega}}\cdot\frac{\partial k}{\partial x_j}\cdot\frac{\partial \omega}{\partial x_j}+\alpha_3\frac{\omega}{k}+p_{wb} \qquad ....(9)$$

The calculation of the individual particle motion was performed using the Discrete Particle Method (DPM). To ascertain the specific movement of each particle, it is necessary to solve equations 10 to 12;

$$\rho_p\frac{du_p}{dt}=F_d+g(\rho_p-\rho)\,!) \qquad \ldots\ldots\ldots (10)$$

The fluid drag force is written as;

$$F_d=\frac{18\mu}{\rho_p d_p^2}\cdot\frac{C_d Re_p}{24}\rho_p(u-u_p) \qquad \ldots\ldots\ldots (11)$$

$$Re_p=\frac{\rho d_{p|u_p-u|}}{\mu} \qquad \ldots\ldots\ldots\ldots (12)$$

The pneumatic sieving chamber was modelled in SolidWorks 2013 as a three-dimensional structure.

Subsequently, the 3D model was loaded into the fluid fluency module of ANSYS 2022. The simulated model has a rotating domain that represents the rotary motion of the shaft and sieve paddles. The domain is contained within the sieve chamber, which represents the region where the sieving process occurs. A frozen type of rotor was selected due to the interaction between the revolving domains and the stationary domains. The single coupled option was employed for the particle interaction (particle coupling). This option enables the transfer of momentum between particles and the continuous phase, allowing the continuous flow to influence the particles. However, the particles themselves are unable to influence the continuous flow. The choice of the single coupled particle interaction was based on its suitability for particles with insignificant masses, such as the wheat particles, due to its well-defined nature. The introduction of the particles into the sieving chamber was accomplished by utilising the particle injection option. In this scenario, the particles were assumed to have a diameter of 35μm and to be uniformly dispersed across the whole inlet surface. A velocity intake was picked at the entrance with a velocity of 4m/s, while a pressure outlet was selected at the exit with a gauge pressure set to 0 Pa.

RESULTS AND DISCUSSIONS

Fluid Velocity in the Sieving Chamber

The fluid velocity distribution inside the sieving chamber, rotating at a speed of 816 rpm, was determined based on the data presented in figure 2. The fluid velocity along the periphery of the sieve chamber appears to be greater than that in other regions. Furthermore, it is evident that the fluid's velocity at the outermost edge of the sieving paddle, which runs parallel to the rotation axis of the sieving shaft, surpasses the velocity of the fluid nearer to the shaft's axis. This is due to the fluid compression exerting pressure on the sieve paddles. The fluid exhibits radial movement as a result of the centrifugal forces exerted on it.

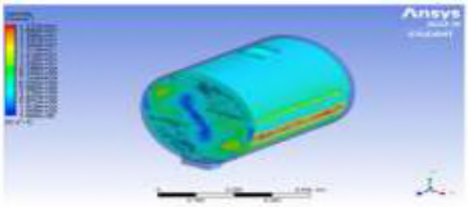

Fig. 2. Fluid velocity distributions at the circumference of sieving chamber

Figure 2 also shows the contour of the fluid velocity distribution around the sieving chamber's circumference. The contour plot allows for the visualisation of the velocity distribution's magnitude across various zones, utilising a predefined colour scheme. The blue zones indicate areas with low velocity. Similarly, the green zones represent areas characterised by moderate velocity, whilst the red zones exhibit the highest velocities.

Figure 2 indicates that the smallest velocity is 0.077 m/s and the maximum velocity is 17.77 m/s.

Figure 3 illustrates the dispersion of velocity contours across different sections of the paddle. The velocity is highest around the perimeter of the sieving chamber and lowest along the axis of the shaft. Figure 4 illustrates the flow of velocity around the sieving shaft and paddles from the intake to the outlet during the sieving operation. The paddles and shaft revolve synchronously at a speed of 816 rpm, inducing a circular motion within the sifting chamber that stirs and propels particles and fluid. Additionally, it was observed that certain particles flow around the shaft and paddles, while others are propelled towards the outside edge of the chamber as a result of centrifugal forces. The fine particles of flour are expelled from the chamber due to the pressure generated by the fleeing velocity, passing through the static sieve net.

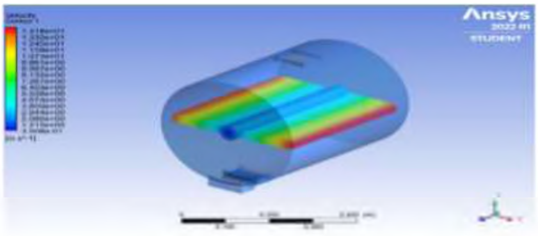

Fig. 3. Fluid velocity distribution on the sieving paddles

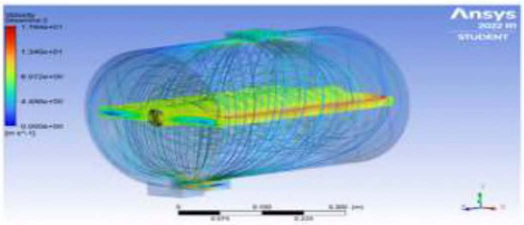

Fig. 4. Fluid velocity stream distribution from inlet to outlet

Fluid Pressure in the Sieving Chamber

Figure 5 indicates that the pressure distribution within the sieving chamber is symmetrical around the shaft axis and progressively increases towards the chamber's outside edge. This condition arises as a result of the paddles acting to draw air from the centre area, which causes a depression in the area where they act. This circumstance is typical, as it indicates that the selected porous domain for the sieve is functioning effectively. At the leading edge of the paddles, where they are rotating, there is an increased pressure. This pressure forces the air, together with the particles of material on the ground, to move in a rotational motion.

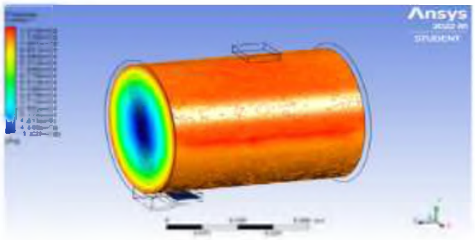

Fig. 5. Fluid pressure on the circumference of the sieving chamber

Turbulence Kinetic Energy

Turbulence within the sieving chamber, as depicted in figure 6, leads to the occurrence of noise and vibration. These specific locations of turbulence are noted below. Turbulence is primarily observed in the discharge region of the sieving chamber, as well as in the area where the paddle is in motion. This is due to the high velocities of the fluid and the restricted space, which forces the movement and dispersion of the material particles inside the sieving chamber and evacuation area.

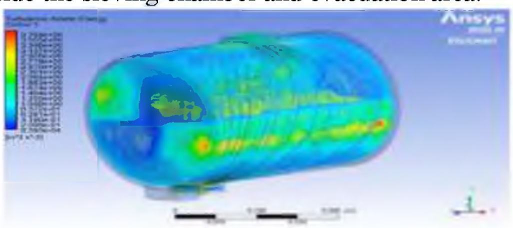

Fig. 6. Turbulence kinetic energy in the sieving chamber

Figure 6 also shows a greater concentration of particles in the input region of the screening chamber. There is another region in the space between the paddle's tip and the sieving chamber where there is a significant concentration of particles. This is because the paddle creates pressure to remove the particles from this location.

Tracking of Flour Particles

Particle tracking involves monitoring the movement of individual particles within a substance. The discrete phase model facilitated the visualisation of particle behaviour within the sieve chamber. Figure 7 and Figure 8 demonstrate that a particle's behaviour is significantly affected by the pressure, air velocity stream, and turbulence kinetic energy within the screening chamber.

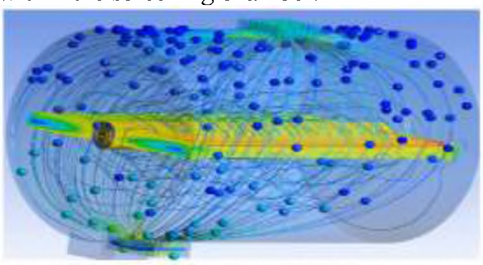

Fig. 7. Particles motion in the sieving chamber

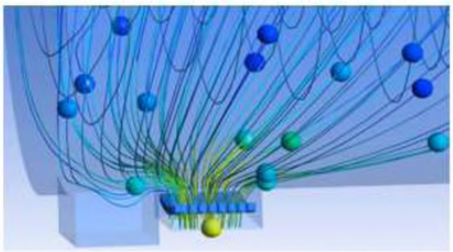

Fig. 8. Particle motion around the sieve net

CONCLUSION AND RECOMMENDATION

Conclusion

The significance of mechanizing traditional food processing techniques in national growth is of utmost importance. Nevertheless, this work employs computational fluid dynamics (CFD) to numerically model the turbo pneumatic sieving process of a bambara flour processing equipment. The aim is to investigate the flow pattern of fluids and particles in the sieving chamber for optimal design of the system.

The study revealed that the behaviour of Bambara flour particles is greatly affected by factors such as pressure, air velocity stream, and turbulence kinetic energy within the sieving chamber.

The CFD-DPM result revealed that the fluid flow and particles motion within the sieving chamber has normal distribution of total pressure. This pressure was shown to increase as particles moves from the axis of the shaft towards the perimeter of the chamber. Additionally, it was observed that the pressure at the leading edge of the sieving paddle is greater than that at the trailing edges. The fluid velocity along the periphery of the sieve chamber is greater than that in other regions. Furthermore, it was observed that the fluid's velocity in front of the paddle is greater than the velocity at the paddle's edge. Turbulence within the sieve chamber primarily occurs in the discharge area as a result of the fluid's high velocities and the confined space in which it is compelled to flow. The turbulence model employed in the CFD simulation demonstrates its ability to accurately forecast the dynamic characteristics of the Bambara flour particles. Therefore, Computational Fluid Dynamics (CFD) is highly effective in accurately forecasting flow patterns and analyzing sieve parameters

Recommendation

Additional research is needed to establish the most effective alignment of the sieving chamber axis in relation to the paddle rotor axis and the discharge chutes in order to improve the removal of flour and chaff material. This will enhance the efficacy of the sieve chamber.

REFERENCES

[1] Atiku A. A., 2000. Bambara groundnut processing and storage practices in North Eastern Nigeria. Maiduguri, Nigeria: University of Maiduguri, Postgraduate seminar, Agricultural and Environmental Resources Engineering Department.

[2] Brough S. H., Azam-Ali S., Taylor A. J. 1993. The potential of Bambara groundnut (*Vigna subterranean*) in vegetable milk production and basic protein functionality systems. Food chemistry, Vol. 47, Issue 3. pp. 277-283. DOI:10.1016/0308-8146(93)90161-8

[3] Ikechukwu. I. F. 2022. Parametric Improvement of Hammer Mill for Bambara Flour Production Using Desirability Optimization Methodology. Nigerian Journal of Technology (NIJOTECH) Vol. 41, No.1., pp. 90-98.

[4] Juliet M., Vinzenco Fogliano, Catherine Chidewe, Anita R. Linnemann 2018. Bambara groundnut (*Vigna subterranea* (L.) Verdc.) flour: A functional ingredient to favor the use of an unexploited sustainable protein source. DOI:10.1371/journal.pone.0205776. pp.1-19.

[5] Ikechukwu I. F., Nwankwojike Bethrand Nduka, Abam Fidelis Ibiam. 2022. Empirical Survey of Postharvest Operations Constraining Bambara Nut Utilization: Proceedings of the 4th African International Conference on Industrial Engineering and Operations Management Nsukka, Nigeria, April 5-7. pp.1-8.
[6] Nachimuthu A.K., Ragunath S., Mohanavelan S., Nab han P.P., Mariraj S. 2016. Design and fabrication of horizontal sand Sieving machine: International Research Journal of multidisciplinary science & Technology, 1(3), pp. 17-20.
[7] Ayoola Olawole Jongbo, Stephen Segun Olajide and Adekunle Temidayo Atta. 2021. The application of computational fluid dynamics (CFD) in the ventilation of agricultural buildings: Journal of Agricultural Engineering and Technology (JAET). Vol. 26., No.1. pp.104-124.
[8] Blocken B. and Gualtieri C. 2012. Ten iterative steps for model development and evaluation applied to Computational Fluid Dynamics for Environmental Fluid Mechanics. Environmental Modelling & Software. Volume 33. pp. 1-22.
[9] Chris Ojiewo, Keatinge J.D.H., Jacqueline d'A. Hughes, Abdou Tenkouano. 2015. The Role of Vegetables and Legumes in Assuring Food, Nutrition, and Income Security for Vulnerable Groups in Sub-Saharan Africa. World medical and health policy Vol. 7, No. 3. pp.187-210
[10] Folasayo T. F., and Zhongjie H., 2019. Computational Fluid Dynamics Modelling of the Heat Pump Drying of Banana: FUOYE Journal of Engineering and Technology. Vol. 4, Issue 2, DOI:10.46792/fuoyejet.v4i2.289. pp.106-111.
[11] Kim R., Lee I., Ha T., Lee S., Lee M., Park G., and Kim J., 2017. Development of CFD model for Predicting Ventilation Rate based on Age. Journal of the Korean Society of Agricultural Engineers, 59(6), pp. 61–71.
[12] Lee I. B., Sase S., and Sung S. H., 2007. Evaluation of CFD accuracy for the ventilation study of a naturally ventilated broiler house. Japan Agricultural Research Quarterly, 41(1), pp. 53–64.
[13] Liu W., Wen J., Lin C., Liu J., Long Z., and Chen Q., 2013. Evaluation of various Categories of turbulence models for predicting air distribution in an airliner cabin. Building and Environment, 65, pp. 118–131.
[14] Mike L. 2016. Different sieving methods for a variety of applications. White paper Series, Retsch GmbH, Solutions in Milling & Sieving, Germany. pp.1-10.
[15] Oh B. W., Lee S. W., Kim H. C., and Seo I. H., 2019. Analysis of Working Environment and Ventilation Efficiency in Pig House using Computational Fluid Dynamics. Journal of the Korean Society of Agricultural Engineers, 61(2), pp. 85–95.
[16] Pragati K., and Sharma H. K., 2012. Concept of Computational Fluid Dynamics (CFD) and its Applications in Food Processing Equipment Design: Journal of Food J Processing & Technology. Vol. 3, Issue 1. DOI: 10.4172/2157-7110.1000138. pp.1-7.
[17] Rohdin P. and Moshfegh B. 2011. Numerical modelling of industrial indoor Environments: A comparison between different turbulence models and supply systems supported by field measurements. Building and Environment, 46(11), pp. 2365–2374.
[18] S. H Brough., S.N. Azam-Ali, A.J. Taylor. 1993. The Potential of Bambara Groundnut (*Vigna Subterranean*) in vegetable milk production and basic protein functionality systems. Food chemistry, Vol. 47, Issue 3. pp. 277-283.
[19] Oyeniyi S. K., Olatunbosun O. S., Aremu A. K., Aviara N. A., Iyilade I. J., 2019. Computational fluid dynamics (CFD) analyses of energy and exergy in thin layer drying of okra (Abelmoschus Esculentus) slices using center shaft rotary tray cabinet (csrtc) dryer: Arid Zone Journal of Engineering, Technology and Environment, September, 2019; Vol. 15(3): ISSN 1596-2490. pp. 762-776.

[20] Terence A., 1981. Particle Size Measurement, Powder Technology Series. Springer Science Business Media, B.V. Third edition. ISBN 978-0-412-15410-2.
[21] Tu J., Yeoh G. H., and Liu C., 2018. Computational fluid dynamics: a practical approach in Elsevier Ltd. (3rd Ed.). Elsevier. pp.1-498.
[22] Aghbashlo M., Mobli H., Rafiee S., and Madadlou A., 2013. A review on exergy analysis of drying processes and systems. Renewable and Sustainable Energy Reviews, 22, pp. 1-22.
[23] Pragati K., and Sharma H. K., 2012. Concept of Computational Fluid Dynamics (CFD) and its Applications in Food Processing Equipment Design: Journal of Food J Processing and Technology. Vol. 3, Issue 1.
[24] Chemmala F., and Dinesh L. R., 2014. Exergy Analysis of Solar Energy Applications and Renewable Energy Systems. International Conference on Advanced Trends in Engineering and Technology, (FORSCHUNG 2014).
[25] Adesoji M. O., Adesoji Matthew Olaniyan, Samuel Kehinde Oyeniyi, Abraham Olusola Oloye, Oluwole Idowu Ogunniyi, Ezinne Winnifred Igwegbe. 2017. Computational fluid Dynamics (cfd) simulation of hot-air flow profile and temperature distribution in a cech dryer: Proceedings of the Int. Food Operations and Processing Simulation Workshop. pp.1-6.
[26] Neil H. Mermelstein. 2016. Sizing up Particles, Food Safety & Quality: Food Technology Magazine. Vol.70., No8.

NUMERIČKO MODELIRANJE TURBO PNEUMATSKOG PROSEJAVANJA ZA PROIZVODNJU BAMBARA BRAŠNA UPOTREBOM RAČUNARSKE DINAMIKE FLUIDA

Ijeoma Francisca Ikechukwu[1], Awa David Onwuka[1], Onyekachukwu James Nwosu[2]

[1]Department of Mechanical Engineering, Michael Okpara University of Agriculture, Umudike, Nigeria
[2]Department of Mechanical Engineering, Gregory University, Uturu, Abia State, Nigeria

Abstract. Polumehanizovana metoda koja je primenjena u preradi Bambara brašna u podsaharskoj Africi ostaje glavno usko grlo u korišćenju Bambara orašastih plodova.

U ovoj studiji, numerički model je upotrebljen za proučavanje i predviđanje karakteristika protoka u turbo pneumatskoj komori za prosejavanje kod nove mašine za preradu brašna Bambare.

Za tu svrhu korišćen je model računarske dinamike fluida (eng. Computational Fluid Dynamics – CFD).

Kao rezultat, testirani su modeli napona smicanja, transporta, velikih i vrtložnih simulacija turbulencije kako bi se model poboljšao. Za simulaciju efekta sita korišćen je porozni efekat. Analizirani su pritisak, brzina fluida i područja turbulencije.

Rezultat analize pokazuje da na proces prosejavanja u velikoj meri utiču pritisak, brzina strujanja vazduha i kinetička energija turbulencije unutar komore za prosejavanje. Poznavanje uticaja pritiska, brzine strujanja vazduha i kinetičke energije turbulencije unutar komore za prosejavanje je od najveće važnosti za poboljšani dizajn ove nove mašine za obradu brašna.

Ključne reči: *Bambara brašno, računska dinamika fluida, simulacija, obrazac strujanja, pneumatsko prosejavanje*

Prijavljen/Registered:
***Submitted*: 26.01.2025.**
Ispravljen:
***Revised*: 01.03.2025**
Prihvaćen:
***Accepted*: 08.03.2025**